

# Mechanical Characterization of Superpave Gradation between Passing through and below Restriction Zone

Tung-Wen Hsu<sup>1</sup>, Wen-Kai Yang<sup>1</sup>, and Jian-Xun Wang<sup>1</sup>

**Abstract:** Mechanical characterization of the Superpave gradations passing through and below the restriction zone is presented through a series of strength tests, which include semi-circular bending test, dynamic modulus test, indirect tensile creep compliance test, indirect tensile fracture energy test, and triaxial shear strength test.

The investigation is firstly to get these two different aggregate structures using Superpave Level 1 mix design method. The optimum asphalt content for the gradation mixtures passing through and below the restriction zone are 5.0% and 4.7%, respectively. The test specimens which were blended at the optimum asphalt content for each gradation mixture were prepared and compacted at four percent of void ratio using Superpave Gyratory Compactor. The Marshall mix design property results indicate that the higher stability values, indirect tensile strength and flow values are observed for the gradation mixtures passing through the restricted zone (TRZ gradation). It appears that these mixtures might possess better resistance against fatigue cracking and less resistance against rutting compared to the gradation mixtures passing below the restricted zone (BRZ gradation). Moreover, the TRZ gradations exhibit the higher fracture toughness in the semi-circular bending tests, the lower exponential values in the creep compliance tests, and the higher fracture energy in the indirect tensile strength tests. All results indicate that the TRZ gradations could have a better capability against fatigue cracking. However, the BRZ gradations reveal the higher dynamic modulus observed at longer reduced time in the dynamic modulus master curves, the more reduced time required to reach the same strain in the repeated loading triaxial tests, and the slightly larger value of  $\phi$  obtained in the triaxial shear tests, all illustrate their superior performance against rutting. Based upon these experimental results, it can be stated that the TRZ gradations exhibit better resistance against fatigue cracking, whereas, the BRZ gradations possess greater performance in rutting resistance.

DOI:10.6135/ijprt.org.tw/2013.6(5).539

**Key words:** *Dynamic Modulus Test; Indirect Tensile Creep Compliance and Fracture Energy Test; Semi-circular Bending Test; Superpave Level 1 mix design.*

## Introduction

Superpave specifies aggregate gradation by adding two features in the mixtures: control points and a restricted zone [1]. A Superpave design aggregate structure is recommended to pass between control points while avoiding the restricted zone. Control points function as master ranges between which gradations must fall. The restricted zone forms a band through which gradations are recommended not to pass. Most designers believe that the BRZ (below restricted zone) gradation passes below the restricted zone could provide a better resistance against permanent deformation compared to the TRZ (through restricted zone) gradation passing through the restricted zone, while some researchers regard that there will be no significant difference or relationship between the BRZ and TRZ gradations on the rutting performance if the crushed aggregate materials are used [2, 3]. Other researches recommend that the restricted zone could be deleted as long as the fine aggregate angularity (FAA) and the volumetric mix criteria meet the minimum requirement (Roberts, et al. 1996) [4]. Since the restricted zone is applied within the fine aggregate sieve sizes, the FAA value seems to become an important

factor affecting the performance of the mixture. Besides, the FAA in central Taiwan is at a value of 45 as described later, which barely meets the minimum requirement for the condition of heavy traffic. Hence, this study is primarily aimed to investigate the effect of the restricted zone on the performance of the mixtures with a margin value of FAA in the fine aggregates.

The objective of this research was firstly to use the Superpave Level 1 mix design method to determine the structure of the Superpave gradations passing through and below the restricted zones, respectively. Subsequently, a series of strength tests which include semi-circular bending test, dynamic modulus test, indirect tensile creep compliance test, indirect tensile fracture energy test, and triaxial shear strength test were conducted on these two different gradation mixtures to evaluate their capability on the resistance of fatigue cracking and rutting.

## Methodology

### Superpave Level 1 Mix Design

Before performing the Superpave Level 1 mix design, it is necessary to select asphalt and aggregate material that meet their respective criteria. The Superpave binder specification is performance based and is selected on the basis of the climate and traffic. Penetration Grade 60/70 of asphalt cement which meets the physical property requirements of high temperature as well as low temperature here in

<sup>1</sup> Department of Civil Engineering, National Chung-Hsing University, Taichung, Taiwan 402.

<sup>+</sup> Corresponding Author: E-mail twhsu@dragon.nchu.edu.tw

Note: Submitted February 18, 2013; Revised June 19, 2013;

Accepted June 20, 2013.

Taiwan is incorporated in this study. The physical properties of Penetration Grade 60/70 of Asphalt Cement were tested and the results are listed in Table 1.

The aggregates were taken from the Wu-Shi riverbed in central Taiwan and the major physical property test results together with the criteria are listed in Table 2. The results indicate that all the consensus aggregate properties meet the criteria, except that the FAA value just fulfills the minimum requirement for the heavy traffic level. It indicates that the fine aggregate particles did not have sufficient amount of fracture faces.

Following Superpave Level 1 design procedures, the trial blends of the mixture gradation [1] were evaluated and the aggregate structures for both BRZ and TRZ gradations of the 19.0 mm nominal mixture are established, respectively as shown in Fig. 1.

After the mixture properties such as air voids, VMA, and VFA are calculated, the design asphalt contents for the BRZ and the TRZ gradation structures are thus determined as 4.7% and 5.0%, respectively. The design mixture properties at design asphalt content as well as the criteria for these two gradation mixtures are shown in Table 3.

### Semi-circular Bending Tests

The energy release rate for a flawed body is valid for linear elastic material behavior. To generalize for the nonlinear elastic materials,

**Table 1.** Physical Properties of Penetration Grade 60/70 of Asphalt Cement.

| Test item   | Value | Specification |
|---|-------|---------------|
| Penetration at 25°C, 100g, 5s (0.1 mm)                      | 66    | 60-70         |
| Flash Point (°C)  | 339   | Min. 232      |
| Ductility at 25°C, 5 cm/min (cm)                            | >100  | Min. 50       |
| Solubility in Trichloroethylene (%)                         | 99.6  | Min. 99       |
| Retained Penetration After Thin-film Oven Test (%)          | 74    | Min. 52       |
| Ductility at 25°C, 5 cm/min, After Thin-film Oven Test (cm) | >100  | Min. 50       |

the concept of path independent *J*-integral was derived by Eshelby [5] and subsequently developed by Rice [6] for its application in fracture mechanics. This test accounts for the resistance of the flawed material to crack propagation. The 150 mm (5.9 in.) by 57 mm (2.25 in.) high cylindrical specimens were prepared using Superpave Gyrotory Compactor and the cylindrical specimens was sliced along their central axes to form two equal semi-circular samples. The semi-circular specimens with different notch depths such as 25.4mm, 31.8 mm and 38.0 mm were fabricated using a saw blade of 3.0 mm thickness. This test was conducted following the test procedures as outlined by Mohammad et al. [7]. A crosshead loading rate of 0.5 mm/min was applied on the specimens until the fracture fail occurred as shown in Fig. 2. During the test, the load

**Table 2.** Physical Properties of Aggregates.

| Test Item                                | Value | Criteria     | Test Method  |
|--|-------|--------------|--------------|
| L. A. Abrasion (%)                       | 19.4  | Max. 30      | AASHTO T 96  |
| Flat and Elongated Particle (%)          | 6.9   | 3:1, Max. 15 | ASTM D 4791  |
|  | 1.4   | 5:1, Max. 5  |              |
| Sodium Sulfate Soundness (%)             |       |              | AASHTO T 104 |
| Coarse Aggregate                         | 0.48  | Max. 12      |              |
| Fine Aggregate                           | 1.71  | Max. 15      |              |
| Coarse Aggregate Angularity              |       |              | ASTM D 5821  |
| Percent Fractured Faces (%): One or More | 100   | Min. 100     |              |
| Two or More                              | 97    | Min. 90      |              |
| Fine Aggregate Angularity (%)            | 45    | Min. 45      | AASHTO TP 33 |
| Sand Equivalent for Plastic Fine (%)     | 79    | Min. 45      | AASHTO T 176 |

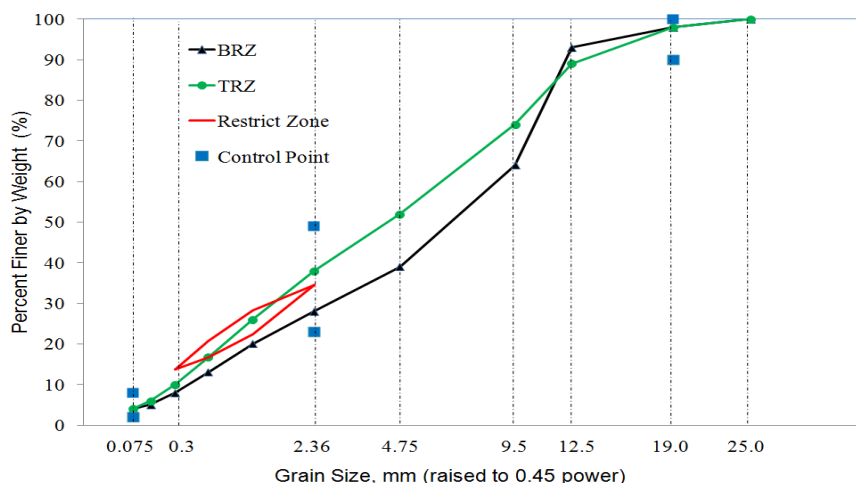


**Fig. 1.** Grain Size Distribution for BRZ and TRZ Gradations.

**Table 3.** Superpave Design Mixture Properties for BRZ and TRZ Gradations

| Mix property               | BRZ  | TRZ  | Criteria     |
|----------------------------|------|------|--------------|
| Design Asphalt Content (%) | 4.7  | 5.0  |              |
| Air Voids (%)              | 4.0  | 4.0  | 4.0          |
| VMA (%)                    | 14.3 | 14.8 | Min.13       |
| VFA (%)                    | 72.1 | 73.0 | 65-75        |
| (% $G_{mm}@N_{ini}=9$ )    | 87.3 | 88.5 | Less Than 89 |
| (% $G_{mm}@N_{max}=205$ )  | 97.3 | 97.1 | Less Than 98 |
| Dust Proportion (DP)       | 0.8  | 1.0  | 0.6-1.2      |



**Fig. 2.** Experimental Setup for Semi-circular Bending Test.



**Fig. 3.** Instrumented Specimen for Dynamic Complex Modulus Test.

and deflection on the specimen were simultaneously recorded and the critical value of *J*-integral (*J<sub>c</sub>*) was determined as follows.

$$J_c = - \frac{1}{B} \frac{\partial U}{\partial a} \tag{1}$$

in which

*J<sub>c</sub>* : fracture toughness, kN·m/mm<sup>2</sup> (lbf·in./in.<sup>2</sup>);

*B* : specimen thickness, mm (in.);

*U* : fracture energy to fail specimen, kN·m (lbf·in.);

*a* : notch depth, mm (in.).

Triplicate specimens were experimented for each individual

mixture and the average test results were used for analysis.

### Dynamic Complex Modulus Tests

The dynamic complex modulus tests were carried out to determine the dynamic modulus of the mixture (ASTM D 3497) [8]. A continuous sinusoidal loading was applied on the mixture and the corresponding deformation was measured. The dynamic modulus is defined as the dynamic stress  $\delta_0$  divided by the recoverable strain  $\epsilon_0$  during the complex modulus test as shown in Eq. (2).

$$|E^*| = \frac{\delta_0}{\epsilon_0} \tag{2}$$

Specimens of four percent air void content with 100 mm (4.0 in.) in diameter and 150 mm (6.0 in.) in height were blended at optimum asphalt content for each gradation mixture and cored from 150 by 150 mm (6.0 by 6.0 in.) specimen using Superpave Gyrotory Compactor. The instrumented specimen was placed inside a triaxial cell which is connected with the actuated piston of the material testing machine as shown in Fig. 3. An air supplied apparatus which provides the desirable confining pressure 206.7 kPa (30 psi) in the confined test was used to pressurize the specimen inside the triaxial cell. Following the testing procedures suggested in the NCHRP 9-19 Report (Witzak et al. 2003) [9], each specimen was conducted with a range of loading frequencies (0.1, 0.5, 1, 5, 10, and 25 Hz) and temperatures (5, 15, 25, 40, and 55°C). Triplicate specimens were tested and the average results were used in the analysis. By using the time-temperature superposition principle, the viscoelastic property of dynamic modulus as a function of time (or frequency) at any temperature can be shifted as a function of reduced time at a desired reference temperature, which is defined in Eq. (3) (Chehab et al. 2002) [10]. After applying the shift factors for different temperature, the master curve of dynamic modulus could be developed and superposed. The detailed analysis for the dynamic modulus master curve and the shift factor can be found in the companion paper (Hsu et al. 2010) [11].

$$t_R = \frac{t}{a_T} \tag{3}$$

in which

*t<sub>R</sub>* : reduced time;

*t* : physical time at a given temperature *T*;

*a<sub>T</sub>* : shift factor for temperature *T*.

In this study, shift factors are determined by fitting a sigmoidal function of the form to the measured dynamic modulus data by using nonlinear least square regression as follows (Pellinen, 2001) [12]:

$$\log|E^*| = a + \frac{b}{1 + \frac{1}{\exp^{(d+e \log f_R)}}} \tag{4}$$

in which

*f<sub>R</sub>* : reduced frequency at the reference temperature;

*a*, *b*, *d*, and *e* : regression coefficients;

$|E^*|$  : dynamic modulus.

In this research, shift factors at reference temperature of 25°C were determined.

**Permanent Deformation of Repetition Loading Test**

The negligible damage specimens which were used in the dynamic modulus tests could be reused in the repeated loading triaxial permanent deformation tests. In this test, a constant vertical stress of 826.8 kPa (120 psi) with a loading frequency of 1 Hz was applied on the specimen in the confined triaxial cell (confining pressure 206.7 kPa (30 psi)) at the temperatures of 25, 40, and 55°C, respectively. The results of accumulated permanent strain versus physical time were simultaneously and continuously recorded until the strain of 4% was reached. Subsequently, the strain was replotted versus reduced time which was converted from physical time by using the time-temperature shift factors obtained from a series of complex modulus tests as discussed in the previous section.

**Indirect Tensile Creep Compliance Tests (Kim and Wen, 2002) [13]**

The creep compliance determined from the indirect tension creep test was used to assess the resistance of the fatigue cracking for the asphalt concrete mixtures. The viscoelastic solution for the creep compliance was developed from the displacements measured on the specimen surface (Kim and Wen 2002) [13]. A set device of displacement measurement was used in this study. Vertical and horizontal LVDTs with gauge length of 50 mm were surface-mounted on both faces of the specimen to eliminate any possible stress concentration of the end effect under the loading strips as shown in Fig. 4. The linear viscoelastic solution for creep compliance  $D(t)$  is (Kim and Wen, 2002) [13] :

$$D(t) = -\frac{d}{P} [\beta_1 U(t) + \beta_2 V(t)] \tag{5}$$

in which

$U(t)$  : horizontal displacement (mm);

$V(t)$  : vertical displacement (mm);

$d$  : specimen thickness (mm);

$P$  : applied load (N);

$\beta_1, \beta_2$  : coefficients which are dependent on gauge length and specimen diameter [13].

To ensure the magnitude of applied load is within the range of linear viscoelastic state during the creep test, the strain was limited to 50-100  $\mu$ . At temperature of 25°C, a crosshead constant load was applied on the specimens for 200 seconds using material testing machine. The creep compliance  $D(t)$  is determined by using Eq. (5) which is based on the average displacement measurement of the vertical and horizontal LVDTs on both faces of the specimen. The test results of  $D(t)$  and time  $t$  were simultaneously recorded and were plotted on double-log of  $D(t)$  versus time  $t$  to get the slope of the exponential  $n$ -value for analysis.

**Indirect Tensile Fracture Energy Tests (Kim and Wen, 2002) [13]**

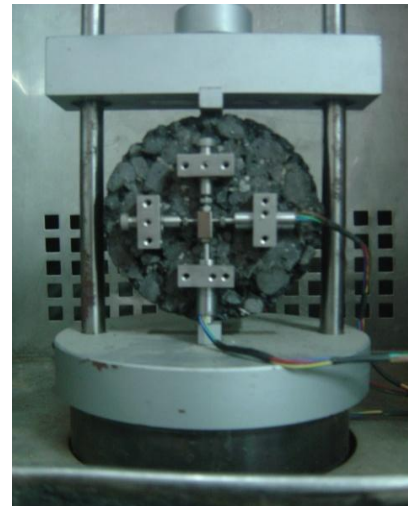


**Fig. 4.** Surface-mounted Vertical and Horizontal LVDTs on Specimen for Indirect Tensile Creep Compliance Tests.



**Fig. 5.** Experimental Setup for Triaxial Shear Strength Tests.

The negligible damaged specimens used in the creep tests were reused in the indirect tensile fracture energy tests. A crosshead loading rate of 75 mm/min. was applied on the specimen until the fracture failure occurred. The center strain  $\epsilon_{x=0}(t)$  and Poisson's ratio  $\nu(t)$  were expressed as [13]:

$$\epsilon_{x=0}(t) = U(t) \frac{\gamma_1 + \gamma_2 \nu(t)}{\gamma_3 + \gamma_4 \nu(t)} \tag{6}$$

$$\nu(t) = -\frac{\alpha_1 U(t) + V(t)}{\alpha_2 U(t) + \alpha_3 V(t)} \tag{7}$$

in which

$\gamma_1, \gamma_2, \gamma_3, \gamma_4, \alpha_1, \alpha_2,$  and  $\alpha_3$  : coefficients which are dependent on gauge length and specimen diameter (Kim and Wen, 2002) [13].

The horizontal tensile stress  $S(t)$  on the vertical diametral plane in the indirect tensile test could be expressed as

$$S(t) = \frac{2P(t)}{\pi D d} \tag{8}$$

in which

$P(t)$  : total applied load during the indirect tensile test (N);

$D$  : specimen diameter (mm).

During the indirect tensile test, the horizontal tensile stress  $S(t)$  and the central strain  $\epsilon_{x=0}(t)$  are simultaneously recorded and plotted in the graph. The fracture energy of the specimen is defined by the area under the stress-strain curve up to the peak stress.

**Triaxial Shear Strength Tests**

The triaxial shear strength test is one of the most reliable methods to determine the shear strength parameters such as cohesion  $c$  and the angle of internal friction  $\phi$  of the soils. The specimen of asphalt concrete mixture was compacted with a dimension of 100 mm (4 in.) in diameter and 200 mm (8 in.) in height using Superpave Gyrotory Compactor. Following the similar test procedures for soil, the specimen was placed inside a plastic triaxial cell with a dimension of 300 mm (12 in.) in diameter and 400 mm (16 in.) in height to accommodate the testing specimen as shown in Fig. 5. At 40°C, the specimens are subjected to a different magnitude of air confining pressure such as 0, 68.95, 137.9, and 206.85 kPa (0, 10, 20, and 30 psi) respectively. Subsequently, an axial vertical deviator stress through a vertical loading ram which is connected to the material testing machine was applied on the specimen until it fails. With the major and minor principal stress at failure for each test, the Mohr’s circles can thus be drawn and the Mohr-Coulomb failure envelopes can be determined as:

$$\tau_f = c + \sigma_f \tan\phi \tag{9}$$

in which

$\tau_f$  : shear strength at failure (kPa);

$c$  : cohesion (kPa);

$\sigma_f$  : normal stress at failure (kPa);

$\phi$  : angle of internal friction (degree).

**Test Results and Discussions**

**Analysis of Mixture Properties Using Marshall Mix Design Criteria**

All the test specimens which were blended at the optimum asphalt content for both BRZ and TRZ gradations were compacted at four percent of void ratio using Superpave Gyrotory Compactor. Following the Marshall mix design method, compacted specimens of both BRZ and TRZ gradations with a dimension of 100 mm (4 in.) in diameter and 63.5 mm (2.5 in.) in height were prepared and tested. The results of mixture properties for both BRZ and TRZ gradations together with the Marshall design criteria were shown in Table 4. The results show that the TRZ gradations exhibit the higher stability values, indirect tensile strength and flow values compared to the BRZ gradations. It suggests that TRZ gradations might possess the better resistance against cracking but less resistance to rutting.

**Semi-circular Bending Test Results**

**Table 4.** Mixture Properties for BRZ and TRZ Gradations with Marshall Design Criteria.

| Test Item                        | BRZ   | TRZ   | Marshall Design Criteria |
|----------------------------------|-------|-------|--------------------------|
| Stability (kgf)                  | 1182  | 1217  | 817                      |
| Flow (0.1mm)                     | 10.5  | 11.3  | 8-14                     |
| Indirect Tensile Strength (kPa)  | 559.8 | 583.5 |                          |
| Tensile Strength Ratio (TSR) (%) | 83.5  | 82.5  | Min. 80                  |

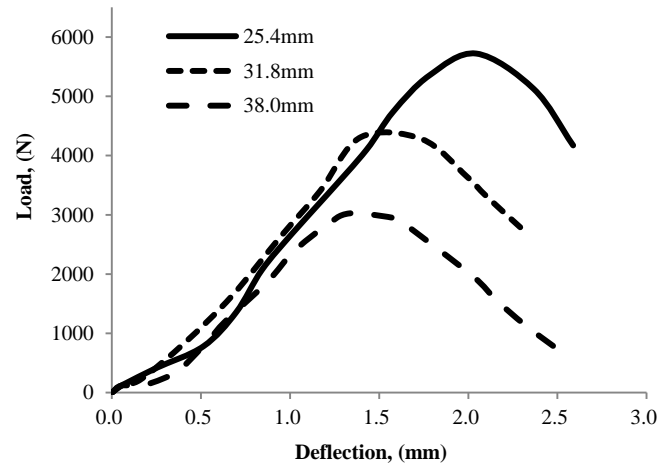


**Fig. 6.** Load-deflection Curve for Different Notch Depths of TRZ Gradation.

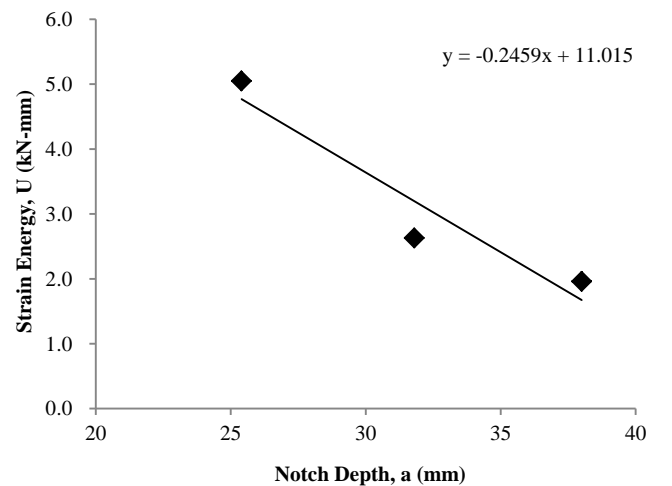


**Fig. 7.** Strain Energy versus Notch Depth for Determining  $dU/da$  of TRZ Gradation.

Specimens with different notch depths of 25.4 mm, 31.8 mm and 38.0 mm were used in this study to determine the fracture toughness of the flawed mixtures. A crosshead loading rate of 0.5 mm/min was applied on the specimens using material testing machine, in addition, the load and the deflection were simultaneously recorded until the fracture failure occurred. The area under the load-deflection curve up to the peak load represents the strain energy  $U$  to fail the specimen as typically shown in Fig. 6. The slope of the strain energy  $U$  versus the notch depth  $a$  through the regression analysis describes the  $\partial U / \partial a$  as plotted in Fig. 7. The critical value of  $J$ -integral

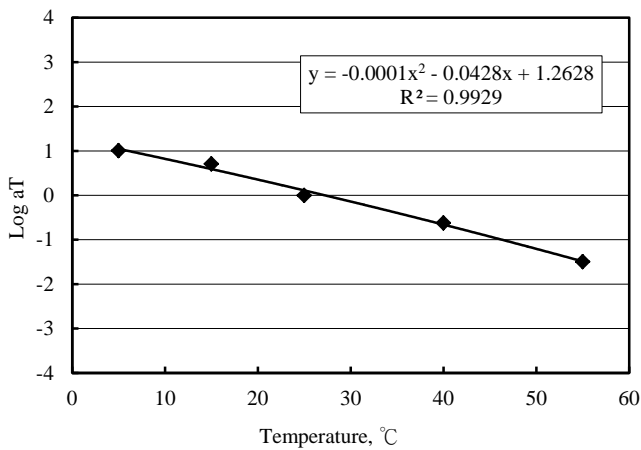


**Fig. 8.** (a) Shift Factor as a Function of Temperature for TRZ Gradation.

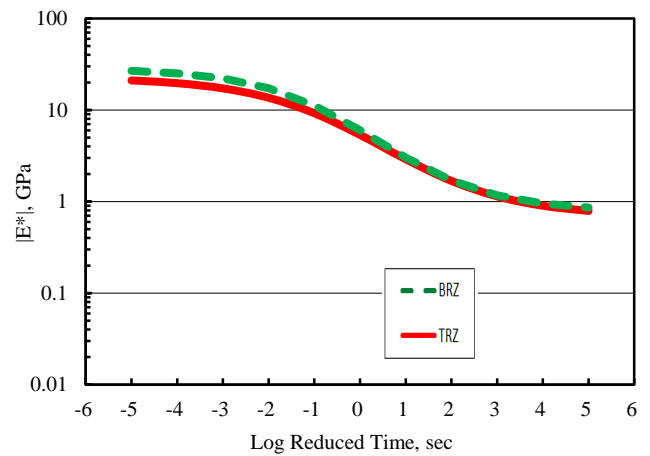


**Fig. 8.**(b) Comparison of Dynamic Modulus Master Curve between BRZ and TRZ Gradation.

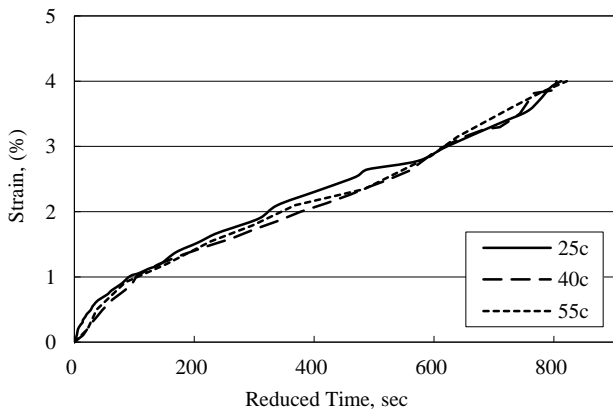


**Fig. 9.**(a) Shifted Accumulated Strain versus Reduced Time of Three Different Temperatures for TRZ Gradation.

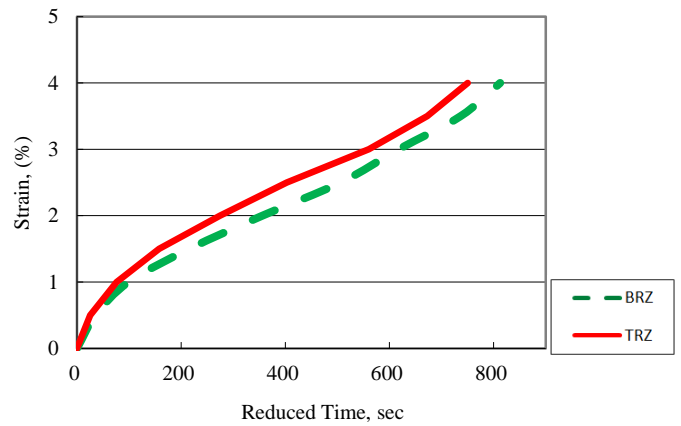


**Fig. 9.**(b) Comparison of Accumulated Strain versus Reduced Time at 25°C between BRZ and TRZ Gradations.

( $J_c$ ) expressed as the fracture toughness was then determined by Eq. (1). Three triplicate specimens were tested for each notch depth and the average test results were used for analysis. The results show that the fracture toughness for the BRZ and the TRZ gradations are 1.27 kJ/m<sup>2</sup> and 4.26 kJ/m<sup>2</sup>, respectively. It indicates that the TRZ gradation might demonstrate the higher resistance against crack propagation.

### Dynamic Complex Modulus Test Results

Dynamic modulus values for each gradation were obtained through a series of dynamic complex modulus tests. Following the time-temperature superposition principles, shift factors as a function of temperature for the TRZ gradation were obtained using Eq. (4) and shown in Fig. 8(a). The dynamic modulus as a function of time at any temperature could then be shifted as a function of reduced time at a desired reference temperature of 25°C to form the dynamic modulus master curve.

The dynamic modulus master curves for both BRZ and TRZ gradations were collected together for comparison as plotted in Fig. 8(b). The results show that the BRZ gradations exhibited the higher dynamic modulus at longer reduced times (higher temperature)

compared to the TRZ gradations. It appears that the BRZ gradation could have better performance against rutting.

### Permanent Deformation of Repetition Loading Test Results

Based on the time-temperature superposition principles, the curves of accumulated permanent strain versus physical time up to a strain of 4% for different temperatures of 25, 40, and 55°C were shifted to the reference temperature of 25°C by using the time-temperature shift factors  $a_T$  obtained from a series of complex modulus tests as described earlier. The test results for all strain histories of the three temperatures are combined into a single strain history on a reduced time scale for the TRZ gradation as shown in Fig. 9(a). For comparison, the average accumulated strain of these three temperatures versus reduced time for both BRZ and TRZ gradations were collected together as shown in Fig. 9(b). The results show that a more reduced time is required to reach the same strain of 4% for the BRZ gradations. It indicates that the BRZ gradations exhibited better resistance against rutting. The results are consistent with the previous findings that the BRZ gradations with higher dynamic modulus at longer reduced time could have better

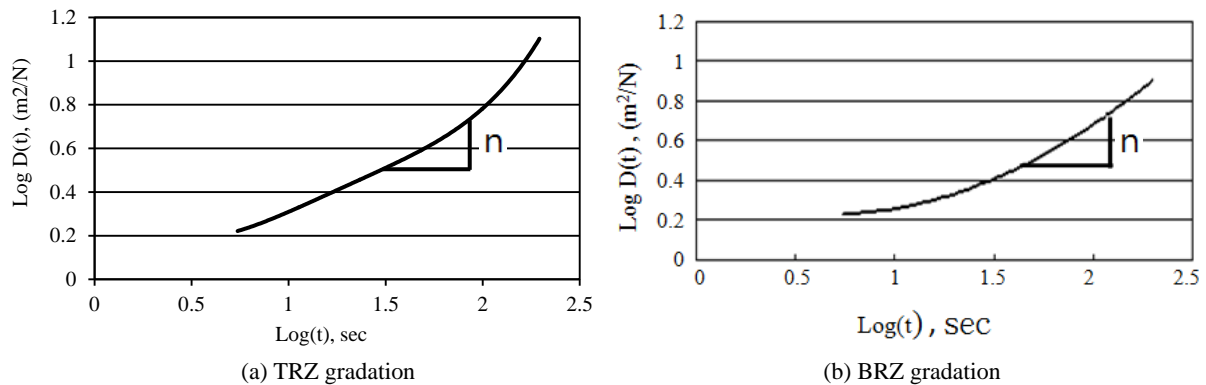


Fig. 10. Exponential *n* Value of Double-log of *D(t)* Versus Time *t*.

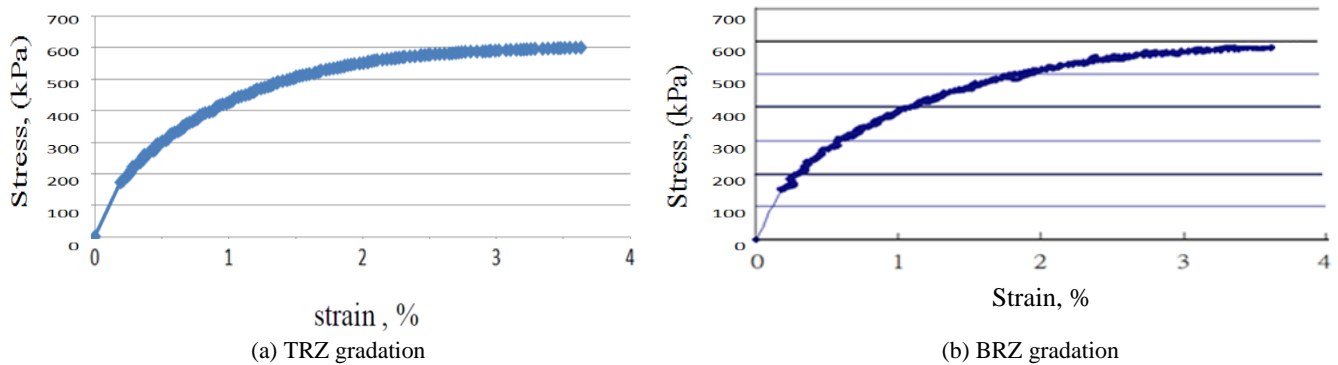


Fig. 11. Stress-strain Curves for Determining Fracture Energy.

resistance against rutting.

**Indirect Tensile Creep Compliance Test Results**

Creep compliance *D(t)* versus time *t* of indirect tensile creep tests for both BRZ and TRZ gradation were determined using Eq. (4) and were plotted on double-log of *D(t)* versus time *t* to get the slope of the exponential *n* value for analysis. The test results for each gradation are shown in Fig. 10(a) and 10(b), respectively. It was found that the TRZ gradations have a lower *n* value of 0.489 compared to the higher *n* value of 0.522 for the BRZ gradation. It suggests that the TRZ gradations could have a better resistance against fatigue cracking (Schapery, 1975) [14].

**Indirect Tensile Fracture Energy Tests**

During the constant loading rate of indirect tensile fracture energy test, the center strain  $\epsilon_{x=0}(t)$  as expressed in Eq. (6) and the horizontal tensile stress *S(t)* in Eq. (8) on the vertical diametral plane were simultaneously recorded until the fracture failure occurs. The stress-strain curves were plotted for both BRZ and TRZ gradations as shown in Fig. 11(a) and 11(b), respectively. The area under the stress-strain curve up to the peak stress was computed, which represents the fracture energy to fail the specimen. The results show that the TRZ gradations have the higher fracture energy of 168.77 kPa compared to the 160.58 kPa for the BRZ gradations. It appears that the TRZ gradations might illustrate the better resistance against fatigue cracking.

**Triaxial Shear Strength Test Results**

Duplicate specimens were conducted by varying the confining pressure of 0, 68.95, 137.9, and 206.85 kPa (0, 10, 20, and 30 psi) during the triaxial shear strength tests, subsequently an axial load was applied until the specimen fails. Mohr’s circles of all tests with different confining pressure were drawn together for each gradation mixture. The Mohr-Coulomb failure envelopes for both gradations were then determined and shown in Fig. 12(a) and 12(b), respectively. The BRZ gradations have the slightly higher value of 42.9° of angle of internal friction compared to the lower value of 42.3° for the TRZ gradations. It indicates that the BRZ gradation might have the higher capacity to develop shear strength under the applied loads, and hence having better resistance against permanent deformation.

**Results and Conclusions**

On the basis of a series of experimental results, the gradation mixtures passing through the restricted zone (TRZ gradation) exhibit the higher fracture toughness found in the semi-circular bending tests, the lower exponential *n* parameter measured in the indirect tensile creep compliance tests as well as the higher values of fracture energy obtained in the indirect tensile strength tests, all indicate that the TRZ gradation could have a better ability against fatigue cracking. However, the gradation mixtures passing below the restricted zone (BRZ gradation) reveal the higher dynamic modulus at longer reduced time obtained in the dynamic modulus master curves, the more reduced time required to reach the same

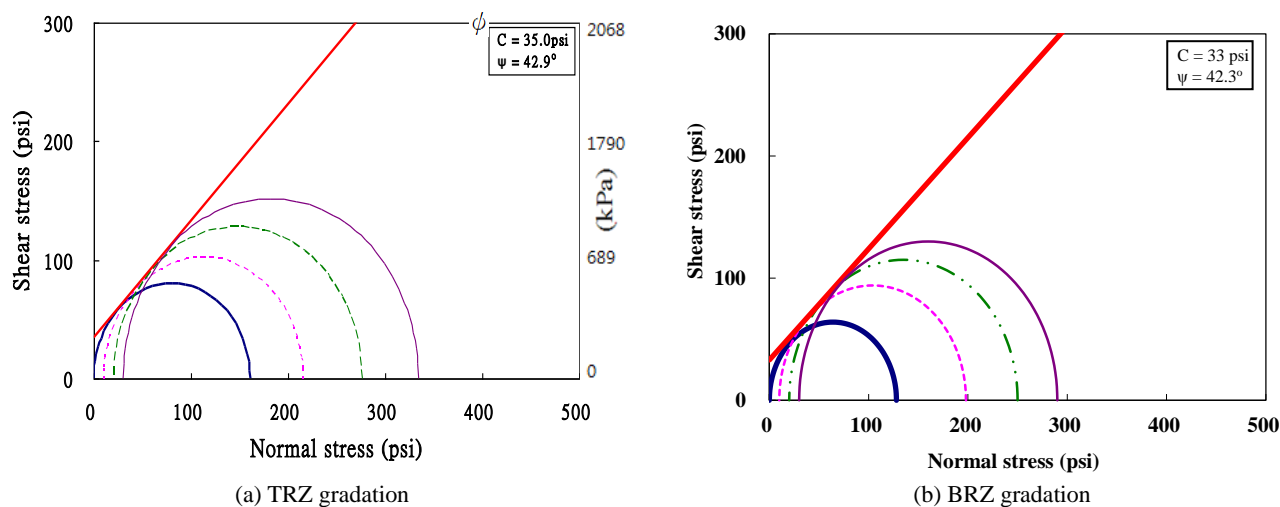


Fig. 12. Mohr-Coulomb Failure Envelope from Triaxial Strength Test.

strain conducted in the repeated loading triaxial tests, and the slightly higher value of  $\phi$  determined in the triaxial shear tests, all illustrate their superior performance against rutting. This study was undertaken to evaluate the mechanical characterization of the gradations passing through and below the restricted zone, with the FAA value of 45 barely meeting the minimum requirement for the condition of heavy traffic. More researches are needed to investigate the aggregates with varying values of FAA on the performance of the mixtures.

### Acknowledgment

This research was sponsored by the National Science Council of Taiwan under Grant No. NSC100-2211-E005-076-MY2. The writers are grateful for the financial support.

### References

- Asphalt Institute (1995). Superpave Level 1 Mix Design, Superpave Series No. 2 (SP-2), Lexington, Kentucky, USA.
- Watson, D.E., Johnson, A., and Jared, D. (1997). The Superpave Gradation Restricted Zone and Performance Testing with the Georgia Loaded Wheel Tester. *Transportation Research Record*, No. 1583, pp. 106-111.
- Kandhal, P. S. and Roberts, A. L. (2002). Investigation of the Restricted Zone in the Superpave Aggregate Gradation Specifications. *Journal of the Association of Asphalt Paving Technologists*, 71, pp. 532-597.
- Roberts, F. R., Kandhal, P. S., Brown, E. R., Lee, D. T., and Kennedy, T. W. (1996). *Hot Mix Asphalt Materials, Mixture Design, and Construction*. Second Edition, NAPA Education Foundation, Lanham, Maryland, USA.
- Eshelby, J. D. (1956). The Continuum Theory of Lattice Defects. *Solid State Physics*, 3, pp. 79-141.
- Rice, J. R. (1968). Mathematical Analysis in the Mechanics of Fracture, Chapter 3 in *Fracture: An Advanced Treatise*, Vol II, Liebowitz, H. (ed.), Academic Press, New York, pp.191-311.
- Mohammad, L.N., Wu, Z., and Aglan, M.A. (2004). Characterization of Fracture and Fatigue Resistance on Recycled Polymer-Modified Asphalt Pavements. *Proceedings of the 5th International Conference*, Limoges, France, pp. 375-382.
- ASTM 3497-79 (1997). Standard Test Method for Dynamic Modulus of Asphalt Mixtures, American Society for Testing and Materials, USA.
- Witczak, T.W., Bari, J., and Quayum, M. (2003). Superpave Support and Performance Models Management, Field Validation of the Simple Performance Test. National Cooperative Highway Research Program, *NCHRP Report No. 9-19*, Arizona State Univ., Tempe, AZ, USA.
- Chehab, G.R., Kim, Y.R., Schapery, R.A., Witczak, M.W., and Bonaquist, R. (2002). Time-Temperature Superposition Principle for Asphalt Concrete with Growing Damage in Tension State. *Journal of the Association of Asphalt Paving Technologists*, 71, pp. 636-684.
- Hsu, T.W., Chen, S.C., and Hung, K.N. (2011). Performance Evaluation of Asphalt Rubber in Porous Asphalt Concrete Mixtures. *Journal of Material in Civil Engineering*, 23(3), pp. 342-349.
- Pellinen, T.K. (2001). Investigation of the Use of Dynamic Modulus as an Indicator of Hot-mix Asphalt Performance. PhD. Dissertation, Arizona State Univ., Tempe, AZ, USA.
- Kim, Y.R. and Wen, H. (2002). Fracture Energy from Indirect Tension Testing. *Journal of the Association of Asphalt Paving Technologists*, 71, pp. 779-793.
- Schapery, R.A. (1975). A Theory of Cracking Initiation and Growth in Viscoelastic Media; Part I: Theoretical Development, Part II: Approximate Methods of Analysis, Part III: Analysis of Continuous Growth. *International Journal of Fracture*, 11, pp. 141-159, pp. 369-388, and pp. 549-562.